



บทความวิจัย

การสาธิตกระบวนการสร้างภาพของฟังก์ชันโดยวิธีของพิกัดทรงกระบอก

พัชรี วงษาสนธิ\* และสุพจน์ สิบบุตร

ภาควิชาคณิตศาสตร์ สถิติและคอมพิวเตอร์ คณะวิทยาศาสตร์ มหาวิทยาลัยอุบลราชธานี

\*Email: patcharee.wo@ubu.ac.th

รับบทความ: 19 พฤศจิกายน 2561 ยอมรับตีพิมพ์: 21 ธันวาคม 2561

บทคัดย่อ

ในงานนี้จะสาธิตกระบวนการสร้างภาพของวัตถุโดยยกตัวอย่างสองตัวอย่าง โดยการจำลองนี้วัตถุนี้จะบรรจุอยู่ในสิ่งปิดที่ไม่สามารถเปิดได้ และจะใช้รังสีที่มีจุดกำเนิดบนเส้นโค้งที่ล้อมรอบสิ่งปิดนั้น ในทางคณิตศาสตร์วัตถุคือฟังก์ชันค่าจริงในสามมิติ สิ่งปิดคือเซตซึ่งมีซัพพอร์ทเป็นเซตกระชับในสามมิติ และจุดกำเนิดรังสีคือเส้นโค้งซึ่งคือเฮลิคซ์ หรือเส้นโค้งอื่นๆ ที่สอดคล้องกับเงื่อนไขที่ทำให้สามารถสร้างภาพได้ และเส้นรังสีคืออินทิกรัลตามเส้นที่มีจุดเริ่มต้นที่จุดกำเนิดรังสี กระบวนการที่ใช้จะใช้พิกัดทรงกระบอกในการหาภาพของฟังก์ชัน ผลที่ได้จะแสดงกระบวนการสร้างระหว่างสองตัวอย่างและการเปรียบเทียบ

**คำสำคัญ:** กระบวนการสร้างฟังก์ชัน จุดกำเนิดรังสี พิกัดทรงกระบอก

อ้างอิงบทความนี้

พัชรี วงษาสนธิ และสุพจน์ สิบบุตร. (2561). การสาธิตกระบวนการสร้างภาพของฟังก์ชันโดยวิธีของพิกัดทรงกระบอก. วารสารวิทยาศาสตร์และวิทยาศาสตร์ศึกษา, 1(2), 134-1421.

Research Article

## Two illustrations of the reconstruction formula in cylindrical coordinate approach

Patcharee Wongsason\* and Supot Seebut

*Department of Mathematics, Statistics and Computers, Ubon Ratchathani University*

*\*Email: patcharee.wo@ubu.ac.th*

Received <19 November 2018>; Accepted <21 December 2018>

---

### Abstract

We provide two demonstrations of reconstruction procedures of objects contained in unopened containers by using rays from a source surrounding them. Mathematically, the objects can be viewed as real-valued functions in three dimensions, the containers as compact support set and the ray source as the helix with radius one. The procedures are in cylindrical coordinate approaches and the results will be shown in two certain functions with comparisons between them.

**Keywords:** Reconstruction procedure, Ray source, Cylindrical coordinate

---

**Cite this article:**

Wongsason, P. and Seebut, S. (2018). Two illustrations of the reconstruction formula in cylindrical coordinate approach. *Journal of Science and Science Education*, 1(2), 134-142.

## Introduction

The studies of viewing an unknown object located inside unopened containers is called computed tomography, namely, recovering tissues inside human bodies or reconstructing velocities of blood flows which are in a study of medical imaging. Mathematically, the tissues or other objects can be thought of as three dimensional real-valued functions  $f : \mathbb{R}^3 \rightarrow \mathbb{R}^3$  and the velocities of blood flows in the latter example as three dimensional vector-valued functions  $g : \mathbb{R}^3 \rightarrow \mathbb{R}^3$  which is in vector field tomography studies. Tomography is used not only in medical imaging but also in atmospheric science, geophysics or oceanography. In this work, we will focus on the former case which is the reconstruction of the real-valued functions.

To achieve the image of  $f$  we place the ray source or a curve surround it and consequently, the source is excited so as to it produces the rays and these rays will pass through the object. The rays will be collected by the detector at the opposite side of the source. The images are produced by processing these collected rays, sometimes called data, with Matlab algorithms. Indeed, we let  $f : \mathbb{R}^3 \rightarrow \mathbb{R}^3$  be a function restricted in a compact support  $\Omega$ . A ray with starting point  $a$  on a curve is the following line integral:

$$\int_0^{\infty} f(a + t\theta) dt, \quad (1)$$

where  $\theta \in S^1$  is the direction of the ray and  $S^1$  denote the set of unit sphere in  $\mathbb{R}^3$ . A visualization of the process is as follow:

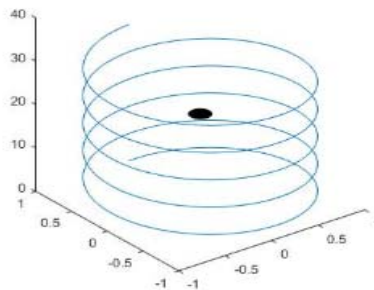


**Figure 1.** A visualization of the reconstruction formula

In figure 1, the black colour represents the object that is of interested in to obtain the image and the helix is the ray source.

One of many procedures, first, uses the inverse Fourier transform and change that setting to spherical coordinate to obtain the rays as in Tuy (1983), Grangeat (1991), Kak & Slaney (1999), Katsevich (2002), Katsevich (2004), and Thongsri et al. (2018). This approach has contributed many reconstruction formulas including the most effective ones, see Katsevich (2002) and Katsevich (2004). In Thongsri et al. (2018) another approach which is the cylindrical coordinate setting has

been proposed and some remarks involving comparisons has been mentioned such as the difference uses of certain functions between them and yet the demonstration has not been shown.

In this work, we will choose two functions:

$$f : \mathbb{R}^3 \rightarrow \mathbb{R}, f(x, y, z) = x^2 + y^3 - z, (x, y, z) \in \mathbb{R}^3$$

and

$$g : \mathbb{R}^3 \rightarrow \mathbb{R}, g(x, y, z) = x^2 + y^3 - z, (x, y, z) \in \mathbb{R}^3.$$

These two functions are examples of three dimensional real-valued functions with different figures, different meanings and also different uses. The results show their images, the analyticities of the processes and comparisons in different uses.

## Objective

To illustrate the reconstruction formula in cylindrical coordinate system by using information from the rays used in the procedures. The illustrations will be shown in two different functions with 3d images, the computations and comparisons with different uses.

## Methodology

For the background, besides Euclidean coordinate in three-dimensional space we introduce two well-known coordinates which are spherical and cylindrical coordinates. The spherical coordinate is a coordinate system that specify a point  $x \in \mathbb{R}^3$  by the radial distance, the polar angle and the azimuth angle. In notation, any  $x$  can be written as

$$x = (r \cos \theta \cos \phi, r \sin \theta \sin \phi, r \sin \theta),$$

where  $0 \leq r \leq \infty$ ,  $0 \leq \theta \leq 2\pi$ ,  $-\pi/2 \leq \phi \leq \pi/2$ , and  $r$  is the radial distance,  $\theta$  is the polar angle and  $\phi$  is the azimuth angle, respectively. This coordinate is appropriated for the 3d object circle-liked shape. Another coordinate is cylindrical coordinate which is the system that any point  $x \in \mathbb{R}^3$  can be expressed as

$$x = (r \cos \theta, r \sin \theta, z)$$

where  $0 \leq r \leq \infty$ ,  $0 \leq \theta \leq 2\pi$ , and  $z$  is the third component in the Euclidean coordinate. Here only polar angle will be used and hence this coordinate is suitable for cylindrical-liked shape or have some rotational symmetry about the longitude axis such as water flow in a straight pipe with round cross-section, blood flow in arteries heat distribution in a metal cylinder.

To obtain the image of any three dimensional real-valued function  $f$ , at a point  $x \in \mathbb{R}^3$  its Fourier transform plays a major role to do so which is

$$\hat{f}(\xi) = \int_{\mathbb{R}^3} f(x) e^{-2\pi i \langle x, \xi \rangle} dx,$$

where  $\langle \cdot, \cdot \rangle$  is the inner product in  $\mathbf{R}^3$ . The Fourier transform is that decompose a function of time into the frequencies relevant to it. It is a tool to reconstruct  $f$  itself via the inverse Fourier transform which is the following:

$$f(x) = \int_{\mathbf{R}^3} \hat{f}(\xi) e^{2\pi i \langle x, \xi \rangle} d\xi. \quad (2)$$

In Tuy (1983), Grangeat (1991), and Katsevich (2002), the process will begin with formula (2) and consequently, the integral will be evaluated in spherical coordinate to gain the rays from the curve. Let  $\Phi$  denote the curve surrounding the compact support of the object. The authors placed the conditions for the curve in order to obtain the effective reconstruction formula as follows:

- 1) The curve is outside the regions.
- 2) The curve is bounded, continuous and almost everywhere differentiable.
- 3) For all  $(x, \beta)$  in  $\Omega \times \mathcal{S}^1$ , there exist  $\lambda$  in  $\Lambda$ , such that  $\langle x, \beta \rangle = \langle \Phi'(\lambda), \beta \rangle \neq 0$ .

Define  $h: \mathbf{R}^3 \times \mathbf{R} \rightarrow \mathbf{R}$  by

$$h(\alpha, \lambda) = \int_0^\infty f(\Phi(\lambda) + t\alpha) dt$$

and  $H$  be its Fourier transform in the first coordinate, i.e.

$$H(\xi, \lambda) = \int_{\mathbf{R}^3} h(\alpha, \lambda) e^{-2\pi i \langle \alpha, \xi \rangle} d\alpha. \quad (3)$$

We observe that  $f$  in the first coordinate is identical to the line integral (1) where the second coordinate tells us the parameter on the curve.

The reconstruction formula for this case is

$$f(x) = \int_0^{2\pi} \int_{-\pi/2}^{\pi/2} \cos \phi \frac{1}{2\pi i \langle \Phi'(\lambda), \beta \rangle} \cdot \frac{\partial H(\beta, \lambda)}{\partial \lambda} d\phi d\theta.$$

In Thongsri et al. (2018), the authors followed same conditions on the curve as in Katsevich (2002) and Katsevich (2004), consequently instead of using the spherical coordinate, they used the cylindrical one and the reconstruction formula has been shown as:

$$f(x) = \int_0^{2\pi} \int_0^{2\pi} H(\beta, \lambda) dz d\theta,$$

where  $\beta = (\cos \theta, \sin \theta, z)$ ,  $0 \leq r \leq \infty$ ,  $0 \leq z \leq 2\pi$  and  $0 \leq \theta \leq 2\pi$ . Here  $\lambda$  is the variable on the curve  $\Phi$  and  $H$  is defined in (3). Moreover, the alternative form of (3) is

$$H(\beta, \lambda) = \int_0^{\infty} r \hat{f}(r\beta) e^{2i\pi \langle \Phi(\lambda), \beta \rangle} dr. \quad (5)$$

## Results

We will demonstrate the procedures of the reconstruction formula in cylindrical coordinate approach with two certain real-valued functions and compare their different uses. The following functions are chosen due to different features and smoothness.

Let us consider the first real-valued function,  $f : \mathbb{R}^3 \rightarrow \mathbb{R}$ , defined by, for  $(x, y, z) \in \mathbb{R}^3$ ,

$$f(x, y, z) = \begin{cases} e^{(x+y-z)} + x - y + z, & \text{if } \|(x, y, z)\|^2 \leq 4 \\ 0, & \text{otherwise} \end{cases}$$

We restricted the function in the region  $-2 \leq x \leq 2$ ,  $-2 \leq y \leq 2$ , and  $-2 \leq z \leq 2$  and the 3d image can be viewed as the following:

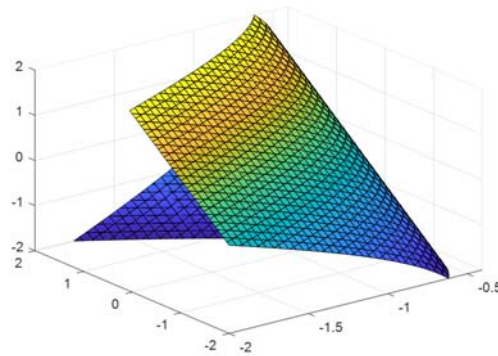


Figure 2. The 3d image of  $f$

The ray in (1) for this case is

$$h_1(y, \theta) = \int_0^{\infty} f(y + t\theta) dt, \quad (6)$$

where  $y$  in the formula is a point on the curve.

The domain of  $f$  leads to the calculation of the ray by considering the inequality

$$\|y + t\theta\|^2 \leq 4.$$

We see that

$$\|y + t\theta\|^2 = t^2(\theta_1^2 + \theta_2^2 + \theta_3^2) + 2t(\theta_1 y_1 + \theta_2 y_2 + \theta_3 y_3) + (y_1^2 + y_2^2 + y_3^2)$$

and since  $\theta$  is a unit vector,  $\theta_1^2 + \theta_2^2 + \theta_3^2 = 1$  and it follows that the limitations of the rays is the solutions of the following quadratic equation

$$t^2 + 2 \langle \theta, y \rangle t + C = 4,$$

Where  $B = \langle \theta, y \rangle$  and  $C = y_1^2 + y_2^2 + y_3^2 = \|y\|^2$ . The solutions to the equation are

$$t_1 = -B - \sqrt{B^2 - (C - 4)}, \quad t_2 = -B + \sqrt{B^2 - (C - 4)}.$$

Therefore, the ray in (6) becomes

$$h_1(y, \theta) = \int_{t_1}^{t_2} \left[ e^{(y_1+y_2-y_3)t + t(\theta_1+\theta_2-\theta_3)} + (y_1 - y_2 + y_3) + t(\theta_1 - \theta_2 + \theta_3) \right] dt. \tag{7}$$

Thus, by integration we obtain

$$h_1(y, \theta) = e^{D+E(t_2-t_1)} + 2D(t_2 - t_1) + \frac{E}{2}(t_2^2 - t_1^2)$$

$$h_1(y, \theta) = e^{D+E(t_2-t_1)} + 2D(t_2 - t_1) + \frac{E}{2}(t_2^2 - t_1^2)$$

and since  $t_2 - t_1 = 2\sqrt{B^2 - (C - 4)}$ ,  $t_2 + t_1 = -2B$ , (7) becomes

$$h_1(y, \theta) = \frac{e^{D+2E\sqrt{B^2-(C-4)}}}{E} + 2D\sqrt{B^2 - (C - 4)} - 2E\sqrt{B^2 - (C - 4)}, \tag{8}$$

where

$$D = y_1 + y_2 + y_3, \quad E = \theta_1 + \theta_2 + \theta_3.$$

The second function that is of interest is

$$g : \mathbb{R}^3 \rightarrow \mathbb{R}, \quad g(x, y, z) = x^2 + y^2 - z^2, \quad (x, y, z) \in \mathbb{R}^3$$

with the same domain as in the first example and its 3d image can be viewed as:

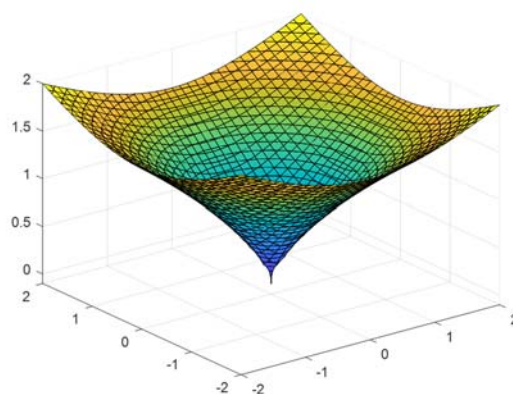


Figure 3. The 3d image of  $g$

Thus, the ray for this function is

$$h_2(y, \theta) = \int_0^{\infty} g(y + t\theta) dt.$$

By using the same calculated fashion as in  $f$ , we obtain

$$\begin{aligned} h_2(y, \theta) &= \int_{t_1}^{t_2} [(y_1 + t\theta_1^2) + (y_2 + t\theta_2^2) - (y_3 + t\theta_3^2)] dt \\ &= \frac{(y_1 + t\theta_1^2)^3}{3\theta_1} + \frac{(y_2 + t\theta_2^2)^3}{3\theta_2} - \frac{(y_3 + t\theta_3^2)^4}{4\theta_3} \Big|_{t_1}^{t_2}. \end{aligned} \quad (9)$$

By substituting  $t_1$  and  $t_2$  into (9),  $h_2(y, \theta)$  reads

$$\begin{aligned} h_2(y, \theta) &= \frac{1}{3\theta_1} [3y_1^2\theta_1(t_2 - t_1) + 3y_1\theta_1^2(t_2^2 - t_1^2) + \theta_1^3(t_2^3 - t_1^3)] \\ &+ \frac{1}{3\theta_2} [3y_2^2\theta_2(t_2 - t_1) + 3y_2\theta_2^2(t_2^2 - t_1^2) + \theta_2^3(t_2^3 - t_1^3)] \\ &- \frac{1}{4\theta_3} [4y_3^3\theta_3(t_2 - t_1) + 6y_3^2\theta_3^2(t_2^2 - t_1^2) + 4\theta_3^2y_3(t_2^3 - t_1^3) + \theta_3^4(t_2^4 - t_1^4)], \end{aligned} \quad (10)$$

where

$$\begin{aligned} t_2 - t_1 &= 2\sqrt{B^2 - (C - 4)} \\ t_2^2 - t_1^2 &= -4B\sqrt{B^2 - (C - 4)} \\ t_2^3 - t_1^3 &= 2\sqrt{B^2 - (C - 4)}(4B^2 - C + 4) \\ t_2^4 - t_1^4 &= -4B\sqrt{B^2 - (C - 4)}(4B^2 - 2(C - 4)). \end{aligned}$$

The results show that  $h_1(y, \theta)$  in (8) has restrictions with the direction  $\theta = (\theta_1, \theta_2, \theta_3)$  which is  $E = \theta_1 + \theta_2 - \theta_3$  must be nonzero and  $h_2(y, \theta)$  in (10) has restrictions with the direction  $\theta = (\theta_1, \theta_2, \theta_3)$  which is each  $\theta_1, \theta_2$ , and  $\theta_3$  must be nonzero. These mean that the restrictions for  $h_1$  is weaker than the restrictions for  $h_2$  because the set of  $\theta$  where each  $\theta_1, \theta_2, \theta_3$  is nonzero is smaller than of the set of  $\theta$  for which  $E \neq 0$ . This leads to the reconstruction of  $f$  is less complicated compare to the reconstruction of  $g$ . One can roughly view that the 3d image of  $f$  is more sophisticated than the one for  $g$ , however, the processes for the reconstruction formula are on the other hand.

## Conclusions

In conclusions, we illustrate the procedures of the reconstruction formula of a real-valued function in three dimensional in cylindrical coordinate approach by showing two different rays used in the processes. The information from the rays tell us how sophisticated of each process is. The rays are produced from two different real-valued functions. The first function viewed for the image



is more complicated than the second one, nevertheless, the process in the reconstruction is simpler than the second one.

### **Acknowledgement**

The images are provided by Matlab licence R2018a: 40692168.

### **References**

- Grangeat, P. (1991). Mathematical framework of cone beam 3D reconstruction via the first derivative of the radon transform (pp 66-97). In G. T. Herman, A. K. Louis and F. Natterer (Eds.), **Mathematical Methods in Tomography** (Vol. 1497). Berlin, Heidelberg: Springer.
- Kak, A. and Slaney, M. (1999). Principles of Computerized Tomographic Imaging. **Classics in Applied Mathematics**. Philadelphia: IEEE Press.
- Katsevich, A. (2002). Analysis of an exact inversion algorithm for spiral cone-beam CT. **Physics in Medicine and Biology**, 47(15), 2583-2598.
- Katsevich, A. (2004). An improved exact filtered Backprojection algorithm for spiral computed tomography. **Advances in Applied Mathematics**, 32(4), 681-697.
- Thongsri, P., Wongsason, P. and Seebut, S. (2018). 3D cone beam reconstruction formula by using cylindrical coordinate. In **Proceeding of Annual meeting in Mathematics 2018** (pp. 41-43). May 3-5 2018, Bangkok.
- Tuy, H. K. (1983). An inversion formula for cone-beam reconstruction. **SIAM Journal on Applied Mathematics**, 43(3), 546-552.